AJNR Am J Neuroradiol 23:368–370, March 2002

Case Report

MR Imaging Characteristics of Amyloid Deposits in Pituitary Adenoma

Steven W. Martin, Daniel R. Lefton, Richard S. Pinto, Marc Rosenblum, and Eric Elowitz

SUMMARY: Although cases of pituitary adenomas containing amyloid deposits have been described in the literature, to our knowledge this is the first report to describe MR imaging characteristics of a pituitary adenoma containing almost entirely amyloid tissue.

Pituitary macroadenomas are one of the more common abnormalities of the sellar region, but reports of such adenomas containing localized amyloid deposits are rare in the literature (1–4). We report a case of pituitary adenoma containing almost entirely amyloid tissue and describe the associated MR imaging characteristics.

Case Report

A 34-year-old man, who reported fertility difficulties of 1-year duration, underwent MR imaging. MR images revealed an intrasellar mass with imaging characteristics consistent with a pituitary adenoma. Hormonal analysis revealed an elevated prolactin level of 199 ng/mL (normal, 2.1–7.7 ng/mL), and the patient was given bromocriptine and then cabergoline for the management of pituitary adenoma. During this time, the diagnosis of insulin-dependent diabetes mellitus was made, and the patient was also treated with 70/30 insulin.

Follow-up MR imaging of the brain was performed with a 1.0-T Vista imager (Picker; Phillips Medical Systems, Highland Heights, OH) 11 months after initiation of medical management of the pituitary adenoma. Images were obtained both before and after the intravenous administration of contrast agent. A mass arising from the pituitary gland measuring 1.3 (anteroposterior) × 2.4 (transverse) × 1.4 (superoinferior) cm and extending into the region of the right cavernous sinus was present. This mass caused expansion of the sella and deviation of the infundibulum to the left. No compression of the optic chiasm was present. The mass was of low signal intensity on T1-weighted images and of even lower signal intensity on T2-weighted images, relative to gray matter. Numerous septations within this mass enhanced after contrast agent administration. However, most of the mass did not enhance (Fig 1).

Because the follow-up images revealed an increase in the size of the tumor, the patient was referred for neurosurgical intervention. Preadmission testing revealed a normal chest radiograph and electrocardiogram, a positive urinalysis for glucose (3+) and trace ketonuria, and a fasting blood sugar of 335 mg/dL. Hormonal analysis revealed a prolactin level (15 ng/mL) and a low testosterone level (46 ng/dL [normal, 241–827 ng/dL]). The patient's 70/30 insulin coverage was increased. A visual single-field analysis threshold test revealed mild circumferential constriction of the right eye, with a pupil diameter of 4 mm and a circumferential constriction of the left eye that was more pronounced nasally with a pupil diameter of 4.9 mm. Both pupils were reactive to light. No visual-field loss was noted at physical examination.

The patient underwent transsphenoidal resection of the pituitary tumor. The contents of the sella were described as firm and calcified. The mass was atypical in appearance for a pituitary adenoma; it could be debulked internally. The patient recovered from the surgery without complications.

Pathologic examination of the tumor revealed nodular congophilic and prolactin-immunolabeled amyloid deposits, a xanthogranulomatous inflammatory reaction, and rare clusters of prolactin-immunoreactive cells (Fig 2). No calcifications were identified. Immunologic findings for adrenocorticotropic hormone, growth hormone, follicle-stimulating hormone, and thyroid-stimulating hormone were negative. These results were consistent with an amyloid-producing prolactinoma with marked degenerative alterations. The paucity of prolactin-secreting cells could be attributed to the medical treatment the patient had been receiving. We recommended that the patient continue medical treatment for the prolactinoma, with surveillance MR imaging.

Discussion

Pituitary macroadenomas are among the more common abnormalities of the sellar region. They originate within the pituitary gland. Usually nonfunctioning, they account for 10–15% of intracranial tumors (5).

Only 13 cases of pituitary adenomas with localized amyloid deposits have been reported in the literature. Amyloid deposits occurred in 41–71% of patients, respectively, in two series of adenomas studied. The incidence varies among the different hormone-secreting types of adenomas and is highest in those secreting growth hormone and prolactin. Two types of amyloid deposits have been reported: spheroid perivascular and stellate perivascular. Stellate perivascular amyloid deposits, the more common type, have a fibrillary or crystalloid microstructure and are usually found along blood vessels. They measure 10−40 μm and are found in all endocrine types of pituitary adenomas (1–4).

The pathologic findings in this case reveal the rare type of amyloid deposit, nodular or spheroid amyloid, which consists of an accumulation of amorphous spheres. These deposits can form coral-like structures. Microscopic examination reveals that the spheres have multilayered concentric substructures that are surrounded by areas containing adenoma cells. Immunoreactive cytokeratin fibrils, which originate in the adenoma cells adjacent to the deposits, are present. Spheroid-type amyloid-containing pituitary adeno-

Received April 3, 2001; accepted after revision August 16.

From the Beth Israel Medical Center (S.W.M., D.R.L., R.S.P., E.E.) and Memorial Sloan-Kettering Cancer Center (M.R.), New York, NY.

Address reprint requests to Daniel Lefton, MD, Beth Israel Medical Center, 170 East End Avenue, 3rd Floor MRI, New York, NY 10128.

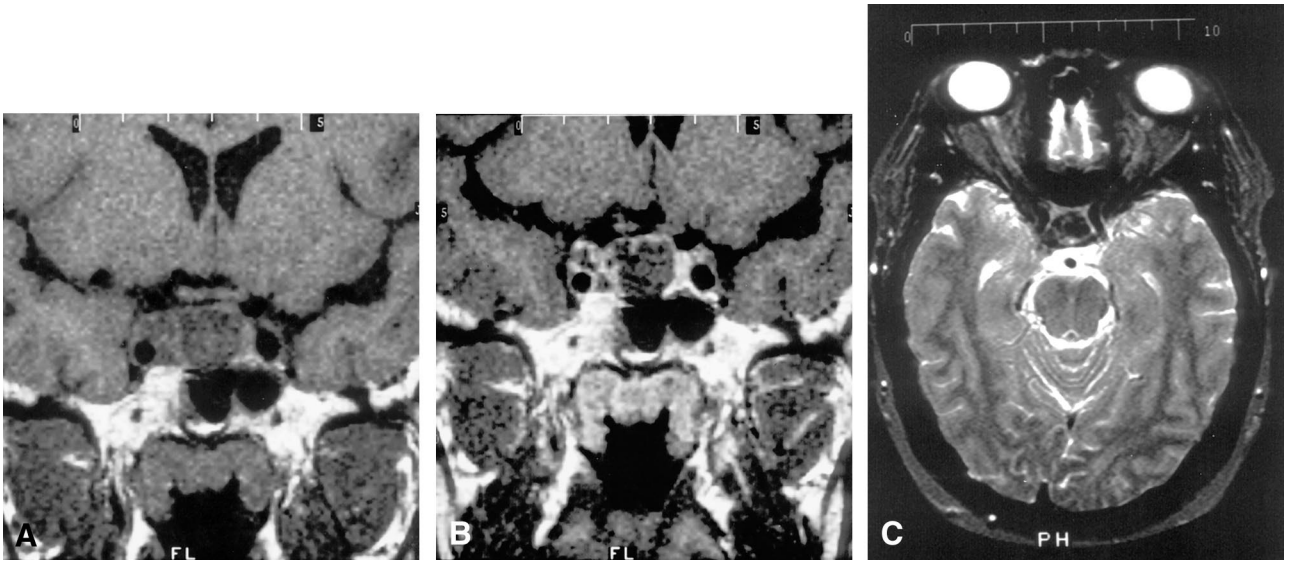

FIG 1. MR imaging of a mass arising from the pituitary gland.
A and *B,* Coronal T1-weighted images of the sella turcica before (*A*) and after (*B*) intravenous contrast agent administration shows an enlarged pituitary gland with expansion of the sella and enhancing intratumoral septations.
C, Axial T2-weighted image through the pituitary shows decreased T2 signal intensity relative to gray and white matter.

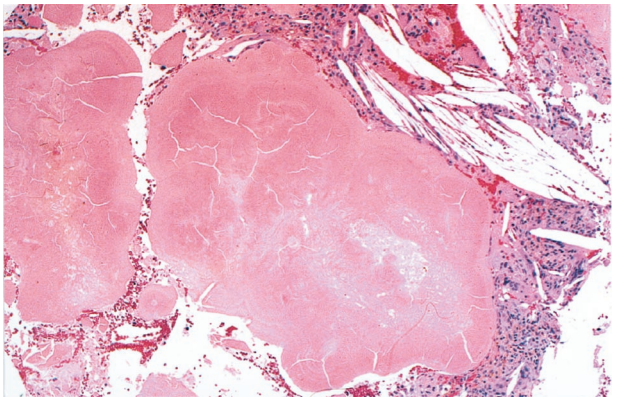

FIG 2. Nodular amyloid deposits are shown as lobulated masses of eosinophilic material with a peripheral, concentric, and ringlike substructure. Cholesterol clefts are seen in the adjacent stroma (hematoxylin-eosin stain, original magnification ×40).

mas are usually suspected or confirmed to be prolactin-producing adenomas (1–3).

The origin of the amyloid deposits have been addressed in various published studies. One suggested possibility is that mesenchymal histiocytes produce the amyloid through an as yet unknown process. These flattened cells have been found to surround amyloid substances. Histiocyte cytoplasm has been noted to contain amyloid fibrils and deposits, and no direct contact between adenoma cells and amyloid fibrils exists. The second theory presented in the literature is that amyloid is produced by adenoma cells, possibly during their degeneration (6). The finding of prolactin-immunoreactive amyloid in our case supports a derivation from adenoma cells.

A study by Saitoh et al (4) suggests that the degradation of secretory granules in vesicles containing amyloid fibrils seems at least partly responsible for the formation of amyloid (4). This same study also revealed that amyloid accumulation is enhanced in adenomas treated with bromocriptine compared with those not treated. This may partly explain the pathologic finding in the specimen of the current case, given the patient's preoperative treatment with bromocriptine (which then increased the amyloid formation).

Contrast-enhanced MR imaging is the accepted diagnostic method for pituitary adenoma, specifically for prolactinoma in patients presenting with elevated prolactin levels (5, 7–9). Signal intensity characteristics enable the differential diagnosis to be narrowed to a limited list of possibilities. These include neoplasms, such as craniopharyngioma, meningioma, germ cell tumor, epidermoid, dermoid, and Langerhans cell histiocytosis; aneurysms; congenital lesions, such as Rathke cleft cysts and arachnoid cysts; and infectious or inflammatory processes, including tuberculosis, meningitis, sarcoidosis, and lymphocytic adenohypophysitis (5, 10). Proper differentiation is of clinical importance, because it will dictate the use of surgical versus nonsurgical treatments (10).

A diagnostic distinction on MR images may be made between pituitary macroadenomas and those containing amyloid deposits. Adenomas usually are isointense relative to gray matter on T1- and T2-weighted images (5). Most tumors enhance intensely and homogeneously. Multilobulated margins are a reliable indicator of an adenoma. Osseous sellar-wall erosion, including extension into the sphenoid sinus or through the dorsum or tuberculum sellae, is typical. This erosion is less common in other masses involving the sellar and suprasellar regions. Displacement of arteries is more common than encasement, which is seen in only 19% of reported macroadenomas (5, 10). The infundibulum can be deviated laterally or upwardly displaced against the inferior hypothalamus (5).

Compression of the optic nerves, tracts, and chiasm may be visualized, although large tumors may obscure these structures due to thinning and displacement. Contrast agent administration may be helpful in separating the optic structures from the tumor; however, it usually is unnecessary in evaluating the extent of the tumor because of contrast enhancement provided by the adjacent cerebrospinal fluid. Hemorrhage occurs in as many as 22% of all pituitary adenomas. An eccentric or central hyperintensity that corresponds to subacute hemorrhage, specifically methemoglobin, is visible on all MR images. Areas of cystic degeneration or necrosis, which have heterogeneous signal intensity characteristics, also may be observed in some macroadenomas. Cysts in necrotic adenomas are hyperintense on T2-weighted images and hypointense on T1-weighted images. Cysts do not enhance after contrast agent administration (5).

To our knowledge, the MR imaging characteristics of a pituitary adenoma containing amyloid deposits has not been described in the literature. We found only one article by Gean-Marton et al (11) that described the MR imaging characteristics of one type of focal amyloidosis of the head and neck. A distinctive loss of signal intensity was noted on T2-weighted images. The authors theorized that the signal intensity loss might reflect static or slowly fluctuating internal magnetic fields arising from adjacent amyloid protons held in relatively fixed positions within the β-pleated sheet. These static or slowly fluctuating internal magnetic fields might then result in quick phase dispersion, chemical exchange, spin-spin interaction with adjacent water protons, and diffusion through differences in diamagnetic susceptibility.

The case presented herein also showed this loss of T2 signal intensity. This characteristic finding of amyloid on MR images may be used to distinguish amyloid-containing pituitary adenomas from those not containing these deposits. This distinction allows more accurate diagnosis and alerts the neurosurgeon that the pituitary tumor has the atypical firm and calcified features.

References

1. Landolt AM, Heitz PU. **Differentiation of two types of amyloid occurring in pituitary adenomas.** *Pathol Res Pract* 1988;183:552–554
2. Bononi PL, Martinez AJ, Nelson PB, Amico JA. **Amyloid deposits in a prolactin-producing pituitary adenoma.** *J Endocrinol Invest* 1993;16:339–343
3. Landolt AM, Kleihues P, Heitz PU. **Amyloid deposits in pituitary adenomas: differentiation of two types.** *Arch Pathol Lab Med* 1987; 111:453–458
4. Saitoh Y, Mori H, Matsumoto K, et al. **Accumulation of amyloid in pituitary adenomas.** *Acta Neuropathol* 1985;68:87–92
5. Hershey BL. **Suprasellar masses: diagnosis and differential diagnosis.** *Semin Ultrasound CT MR* 1993;14:215–231
6. Kuratsu J, Matsukado Y, Miura M. **Prolactinoma of pituitary with associated amyloid-like substances.** *J Neurosurg* 1983;59:1067–1070
7. Magnaldi S, Frezza F, Longo R, Ukmar M, Razavi IS, Pozzi-Mucelli RS. **Assessment of pituitary microadenomas: comparison between 2D and 3D MR sequences.** *Magn Reson Imaging* 1997;15: 21–27
8. Rand T, Kink E, Sator M, et al. **MRI of microadenomas in patients with hyperprolactinaemia.** *Neuroradiology* 1996;38:744–746
9. Kobayashi S, Ikeda H, Yoshimoto T. **A clinical and histopathological study of factors affecting MRI signal intensities of pituitary adenomas.** *Neuroradiology* 1994;36:298–302
10. Donovan JL, Nesbit GM. **Distinction of masses involving the sella and suprasellar space: specificity of imaging features.** *AJR Am J Radiol* 1996;167:597–603
11. Gean-Marton AD, Kirsch CF, Vezina LG, Weber AL. **Focal amyloidosis of the head and neck: evaluation with CT and MR imaging.** *Radiology* 1991;181:521–525